10-10-1975

Theoretical Single-Domain Grain Size Range in Magnetite and Titanomagnetite

Robert F. Butler
University of Portland, butler@up.edu

Subir K. Banerjee

Theoretical Single-Domain Grain Size Range in Magnetite and Titanomagnetite

ROBERT F. BUTLER

Department of Geosciences, University of Arizona, Tucson, Arizona 85721

SUBIR K. BANERJEE

Department of Geology and Geophysics, University of Minnesota, Minneapolis, Minnesota 55455

A theoretical model of single-domain (SD) grain sizes is applied to magnetite and titanomagnetite. In this model, transition to a two-domain configuration takes place at the SD threshold d_0. This two-domain configuration is shown to be more applicable to fine-grained magnetites in igneous rocks than previous models involving transition to a circular spin configuration at d_0. Calculations of the stable SD grain size range were accomplished by calculating the superparamagnetic threshold size d_s by Néel's relaxation equation and calculating the SD threshold d_0 at which SD to two-domain transition occurs. For cubic magnetite particles the SD range is extremely narrow and occurs at very small grain size. At room temperature, $d_s \simeq 0.05$ μm, and $d_0 \simeq 0.076$ μm. For cubic magnetite particles just above d_0 a two-domain configuration is predicted in which a 180° domain wall occupies ~60% of the particle volume. No SD range exists for cubic magnetites at $T > 450$°K. These results are in good agreement with experimental determinations of SD limits in equant magnetites and also agree with experimental observations of thermoremanent magnetization in submicron pseudo-single-domain (PSD) magnetites. The SD range increases rapidly with particle elongation. For a length:width ratio of 5:1, SD limits of $d_s \simeq 0.05$ μm and $d_0 \simeq 1.4$ μm are calculated. Both d_0 and the SD range for titanomagnetites ($Fe_{3-x}Ti_xO_4$) increase with Ti content. For cubic titanomagnetites of $x = 0.6$, $d_s \simeq 0.08$ μm, and $d_0 \simeq 0.3$ μm. Comparison of the calculated SD range with the available high-resolution grain size distributions of opaque grains in igneous rocks suggests that elongated SD grains or submicron PSD grains are the major carriers of stable natural remanence in igneous rocks.

INTRODUCTION

Single-domain (SD) grains are known to be efficient and stable carriers of thermoremanent magnetization [*Néel*, 1949]. Thus SD magnetite is an attractive candidate for the carrier of stable natural remanent magnetization (NRM) in igneous rocks. However, SD behavior occurs only within a narrow grain size range. Below the superparamagnetic (SP) threshold grain size d_s, thermal activation destroys the remanence-carrying capability of the particle. Above the single-domain threshold size d_0 a nonuniform spin structure develops in which the atomic magnetic moments are no longer parallel throughout the particle. The stable SD range between d_s and d_0 for cubic magnetite grains is very narrow and occurs at grain sizes of $\ll 1$ μm [*Néel*, 1955]. Because the grain size distributions of optically visible magnetite in igneous rocks generally peak at >1 μm, *Stacey* [1963] concluded that the predominant carriers of remanence were pseudo-single-domain (PSD) grains just above the SD size.

Recent evidence has led to a resurgence of interest in the magnetic properties of SD and submicron magnetite [*Evans*, 1972]. Since SD magnetite is below the optical line of resolution, there is little direct evidence for its presence in igneous rocks. However, several careful studies of magnetic properties of mineral separates from intrusive rocks have provided indirect evidence that the stable NRM resides in single-domain grains rather than in larger optically visible oxides [e.g., *Evans et al.*, 1968; *Evans and McElhinny*, 1969; *Hargraves and Young*, 1969; *Murthy et al.*, 1971]. *Evans and Wayman* [1970] have used electron microscopy to examine submicron magnetite and have observed particles which are within the expected SD grain size limits. *Larson et al.* [1969] have also suggested that the proportion of submicron magnetites in igneous rocks is commonly underestimated. These observations indicate that SD magnetite is an important, if not dominant, contributor to stable NRM in many igneous rocks. Thus delineation of the stable SD grain size limits for magnetite is an important problem in paleomagnetism.

Experimental examinations of equant submicron magnetite particles have been undertaken by *Dunlop* [1972, 1973*a*, *b*]. Values of 0.03 and 0.05 μm were found for d_s and d_0, respectively. Extension of experimental determinations of d_s and d_0 to elongated magnetite particles would be very difficult, if not impossible. Particles with a very narrow shape and grain size distribution would be required. Thus a theoretical treatment of single-domain grain size limits for elongated (as well as equant) magnetite particles is desired.

A related problem is the investigation of pseudo-single-domain behavior. Magnetite particles with a grain size between SD and true multidomain (MD) size (~17 μm) exhibit hysteresis properties similar to MD grains but are capable of carrying remanence whose intensity and coercivity are similar to those of SD grains [*Parry*, 1965]. *Stacey* [1963] and *Dickson et al.* [1966] have attributed the origin of PSD behavior to Barkhausen discreteness of domain wall position. *Stacey and Banerjee* [1974, p. 110] have proposed that PSD moments occur at the surface terminations of domain walls. Thus the observation of pseudo-single-domain behavior seems to require the presence of domain walls in submicron magnetite above SD size. Moreover, *Dunlop* [1973*b*] has recently shown that the TRM characteristics of submicron magnetite are best explained by the development of a two-domain structure at d_0 in which a 180° domain wall occupies ~50% of the particle volume. Any theoretical treatment of SD magnetite must not

only be consistent with the experimentally observed d_s and d_0 for equant particles but must also account for the development of PSD behavior.

Theoretical calculations of single-domain limits have been reviewed by *Evans* [1972]. The presently favored theory is that of *Morrish and Yu* [1955] in which a SD to circular spin transition takes place at d_0. However, the Morrish and Yu theory considers only ellipsoidal particles. Direct observations of submicron magnetite in igneous rocks indicate that these particles are not ellipsoidal but rather are bounded by crystal faces [*Evans and Wayman*, 1970]. Thus the applicability of the Morrish and Yu theory of SD magnetite in igneous rocks is questionable. Also, transition to a circular spin configuration (with no net magnetic moment) at d_0 does not seem consistent with the development of PSD behavior. Therefore a theoretical treatment which considers parallelepiped-shaped particles and involves the development of domain structure at d_0 would seem more appropriate for SD magnetite in igneous rocks.

In this paper we examine a theoretical treatment of parallelepiped-shaped particles containing a single 180° domain wall. This theory was developed by *Amar* [1957, 1958*a*, *b*] and applied to calculations of SD limits in metallic iron. The energetics of the *Morrish and Yu* [1955] circular spin configuration and the two-domain configuration of *Amar* [1958*a*] will first be introduced. We conclude that the two-domain arrangement is appropriate for fine magnetite particles in igneous rocks. This conclusion is an important reconciliation between theory and experiment. The SD grain size limits for elongated magnetite are then calculated, and their implications are discussed. Single-domain threshold sizes for titanomagnetites are also calculated and shown to be consistent with observations.

Circular Spin Configuration

The calculations of *Morrish and Yu* [1955] considered the exchange energy of the circular spin configuration in ellipsoidal particles of magnetite and maghemite. Magnetocrystalline anisotropy energy was neglected. In an ellipsoidal particle the circular spin configuration produces no free magnetic poles, and there is no magnetostatic energy. However, in a particle bounded by crystal faces the circular spin arrangement will produce a complicated surface density of free magnetic poles. These surface charges will result in considerable magnetostatic energy. Both the neglected magnetocrystalline anisotropy energy and the magnetostatic energy of the circular spin configuration in a parallelepiped are discussed below.

In order to investigate the seriousness of neglecting magnetocrystalline anisotropy energy we can calculate the anisotropy energy of a particular circular spin configuration and compare the calculated energy with the exchange energy at the critical size d_0. The assumed unimportance of the anisotropy energy is valid only if the anisotropy energy is negligible in comparison to the exchange energy.

The neglected anisotropy energy per unit volume e_K for a prolate ellipsoid elongated parallel to [001] was found to be $e_K = 5K_1/24$, where K_1 is the first-order anisotropy constant. Details of this calculation are given in Appendix 1. If a circular spin configuration develops at d_0, the energy of this nonuniform configuration must equal the single-domain energy e_{SD} at the critical size. The SD energy per unit volume is simply the magnetostatic energy given by

$$e_{SD} = \tfrac{1}{2}N_D J_s^2 \qquad (1)$$

where N_D is the self-demagnetizing factor and J_s is the saturation magnetization (=480 emu/cm³ for magnetite at room temperature). For a spherical particle, $N_D = 4\pi/3$. Using $K_1 = 1.3 \times 10^5$ ergs/cm³ from *Fletcher and O'Reilly* [1974], we find $e_K/e_{SD} = 0.06$ for a spherical particle. For a prolate ellipsoid with elongation of 2.5 the demagnetizing factor along the polar axis is 1.7 [*Morrish*, 1965, p. 10], and $e_K/e_{SD} = 0.14$. The neglected magnetocrystalline energy is not negligible and will have the effect of increasing the calculated d_0 values based on the theory of *Morrish and Yu* [1955].

A more serious objection to the circular spin arrangement arises if we consider the magnetostatic energy produced by this configuration when it is confined to a parallelepiped-shaped particle. This objection is not a criticism of the calculations of *Morrish and Yu* [1955] but does raise questions as to the application of this theory to the fine-grained magnetites of igneous rocks. These submicron magnetite particles are bounded by crystal faces and are certainly more parallelepiped than ellipsoidal. The magnetic charge distribution resulting from confining the circular spin configuration in a parallelepiped is schematically illustrated in Figure 1. A general expression for the magnetostatic energy E_m is given by *Brown* [1963*a*] as

$$E_m = -\frac{1}{2}\int \mathbf{J}\cdot\mathbf{H}'\, dv \qquad (2)$$

where $\mathbf{J}$ is the magnetization vector, which is a function of position, and $\mathbf{H}'$ is the internal demagnetizing field, which is also dependent on position in the particle. The internal demagnetizing field $\mathbf{H}'$ is produced by the volume charge density $\rho_m = -\nabla \cdot \mathbf{J}$ and surface density $\sigma_m = \hat{n} \cdot \mathbf{J}$, where $\hat{n}$ is a unit vector normal to the surface. For the charge distribution shown in Figure 1, $\mathbf{H}'$ would be a complicated function of position, and a rigorous derivation of the magnetostatic energy would be very difficult. However, a rough estimate of this magnetostatic energy can be accomplished by allowing several approximations.

The surface charges illustrated in Figure 1 are concentrated along the faces of the prismatic regions at the corners of the parallelepiped. The magnetostatic energy of these prisms can be estimated by considering them to be uniformly magnetized parallel to the hypotenuse of their triangular cross section. These uniformly magnetized prismatic regions are also shown in Figure 1. The self-demagnetizing factor inside a uniformly magnetized right triangular prism is a complicated function of position. However, the demagnetizing factor perpendicular to the axis of a prism with an equilateral cross section is independent of position [*Moskowitz and Della Torre*, 1966]. Thus further approximation of the right triangular prisms of Figure

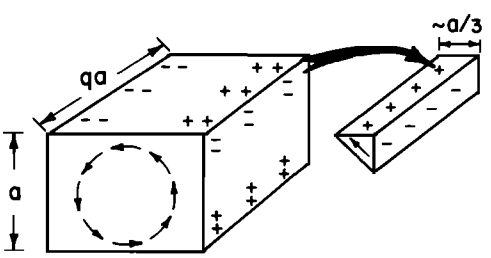

Fig. 1. Circular spin configuration in a parallelepiped. The magnetic charge distribution resulting from confining the circular spin configuration in a parallelepiped is schematically illustrated in the left diagram. Prismatic regions of concentrated magnetic charges and approximate uniform magnetization are shown in the right diagram. See text for estimate of the magnetostatic energy.

1 by equilateral triangular prisms will facilitate an estimate of the magnetostatic energy.

If the parallelepiped has a square cross section of width a and length qa, where q is elongation, the prismatic regions will have length qa, and the sides of the equilateral triangular cross section will be $\sim a/3$. The demagnetizing factor perpendicular to the axis of the equilateral prism is $\sim 1.75\pi$ for $q = 1.0$ and $\sim 1.88\pi$ for $q = 2.5$ [*Moskowitz and Della Torre*, 1966]. The magnetostatic energy E_M of the prism is

$$E_M = \tfrac{1}{2} N_D J_s^2 v \tag{3}$$

where v is the volume of the prism and is equal to $qa^2 \sin(60°)/18$. For a cubic particle with $q = 1.0$ the total magnetostatic energy of the four prisms is

$$4E_M = 0.168\pi a^3 J_s^2 \tag{4}$$

Where this is used as an approximation of the magnetostatic energy of a cubic particle containing the circular spin arrangement, the magnetostatic energy per unit volume e_M is $0.168\pi J_s^2$. The single-domain energy e_{SD} is simply $(2\pi/3)J_s^2$, and $e_M/e_{SD} \simeq 0.25$. Thus the magnetostatic energy resulting from the circular spin configuration in a cubic particle is ~25% of the single-domain energy. For a particle of elongation $q = 2.5$ a similar calculation yields $e_M/e_{SD} \simeq 0.55$, and the magnetostatic energy of the circular spin configuration in a parallelepiped of $q = 2.5$ is ~50% of the SD energy. Application of the *Morrish and Yu* [1955] calculations to magnetite particles of igneous rocks amounts to neglecting this large energy contribution. Although the distribution of magnetization may readjust in order to decrease the magnetostatic energy, any such readjustment must be done at the expense of increased exchange energy.

The above estimates do not rigorously prove that the circular spin arrangement is inappropriate for the desired SD calculations. However, these arguments should be sufficient incentive to develop a theoretical treatment which is designed for parallelepipeds rather than ellipsoidal particles.

TWO-DOMAIN CONFIGURATION

Kittel [1949] attempted to determine d_0 for metallic iron by comparing the single-domain energy with the magnetostatic and wall energy of a two-domain particle. This derivation assumed that the 180° domain wall width was negligible in comparison with the particle size. However, the calculation led to the paradoxical result that the predicted d_0 (~0.02 μm) was less than the 180° wall width (~0.1 μm). *Stacey* [1963] obtained the same paradoxical result when appropriate values for magnetite were substituted into *Kittel*'s [1949] derivation.

Amar [1957, 1958*a*, *b*] has significantly improved these calculations by considering two important refinements of Kittel's derivation. First, Amar observed that the surface terminations of the domain wall would produce free magnetic poles and resulting magnetostatic energy which had previously been neglected. Second, Amar included the dependence of domain wall energy on the wall width. The two-domain plus 180° wall configuration is illustrated in Figure 2. Although the calculations of magnetostatic and wall energy for this configuration are somewhat involved, the basic idea is simple. The magnetostatic energy of the two-domain configuration is much less than that for a uniformly magnetized SD parallelepiped. In order to decrease the high magnetostatic energy of the SD configuration, a 180° domain wall is reduced in width and introduced between two oppositely magnetized domains. The energy/unit area of this 180° wall is increased when it is

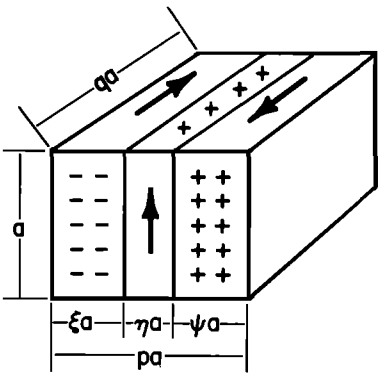

Fig. 2. Two-domain configuration. The parallelepiped is partitioned into two domains with an intervening domain wall. Directions of magnetization are shown by the arrows, while the plus and minus symbols indicate the equivalent surface charge distribution. Particle height is a, width is pa, length is qa, and domain wall width is ηa.

reduced in width. However, above the critical SD size d_0 the total energy of the two-domain configuration is less than the SD energy. In this way, domain structure can develop in particles whose size is less than the equilibrium domain wall width in the extended medium.

As with any theoretical treatment, several simplifying approximations are required to make the problem tractable. The most obvious assumption employed in this two-domain theory is that the particles are parallelepipeds as shown in Figure 2. This assumption is necessary in order to allow calculation of the magnetostatic energy. Although the exact shape of submicron magnetites in igneous rocks will not be a perfect parallelepiped, this shape is much closer to reality than the ellipsoidal shapes considered by *Morrish and Yu* [1955].

Another approximation is that the domain wall has sharp boundaries as illustrated in Figure 2. The direction of magnetization is assumed to change sharply by 90° at either side of the wall. This assumption is also required to make the calculation of the magnetostatic energy manageable. In reality, the direction of magnetization will rotate over a finite distance. The effect of this approximation will be to overestimate the magnetostatic energy of the 180° domain wall. This overestimate will be most serious for elongated particles in which the direction of magnetization in the domain wall is perpendicular to the elongation and thus along a direction of high demagnetizing factor. The inflated magnetostatic energy will in turn lead to calculated wall thickness in elongated particles which are slightly less than would be calculated by using a magnetization distribution which rotates through the wall. Since the demagnetizing factor is invariant with direction within a cube, the calculated wall thickness in a cube will not suffer this reduction.

The magnetostatic energy of the two domains and the domain wall can be calculated using the *Rhodes and Rowlands* [1954] theory of demagnetizing energies in uniformly magnetized rectangular blocks. Normalizing the total magnetostatic energy E_m of the two-domain particle by dividing with $2a^3J_s^2$ yields the 'reduced' magnetostatic energy $e_m \doteq E_m/2a^3J_s^2$, where a is the particle width. The reduced magnetostatic energy of the configuration shown in Figure 2 was derived by *Amar* [1958*a*] and is given by

$$\begin{aligned} e_m = q[&-pg(p, q) - \eta g(\eta, q) + (\xi + \eta)g(\xi + \eta, q) \\ &+ (\eta + \Psi)g(\eta + \Psi, q) + \xi g(\xi, q) \\ &+ \Psi g(\Psi, q) + \eta g(\eta/q, 1/q)] \end{aligned} \tag{5}$$

where

$$g(p, q) = [F(p, 0) - F(p, q)]/[pq] \quad (6)$$

and $F(p, q)$ is the *Rhodes and Rowlands* [1954] function whose complete expression is given in Appendix 2.

For a particle of square cross section, $p = 1$, and for equal volume domains (as expected for no strong external field), $\xi = \Psi = (1 - \eta)/2$. Thus (5) reduces to

$$e_m = q\{-g[1, q] - \eta g[\eta, q] + [1 + \eta]g[(1 + \eta)/2, q] + [1 + \eta]g[(1 - \eta)/2, q] + \eta g[(\eta/q), (1/q)]\} \quad (7)$$

Equation (7) allows calculation of reduced magnetostatic energy e_m in terms of the particle elongation q and fraction of particle width η occupied by domain wall.

The dependence of the domain wall energy σ on the wall width δ is given by

$$\sigma = (\sigma_0/2)(\delta/\delta_0 + \delta_0/\delta) \quad (8)$$

where σ_0 and δ_0 are the wall energy and wall width in the extended medium [*Amar*, 1958*a*]. With domain wall area of qa^2 and wall width $\delta = \eta a$ the domain wall energy E_w is

$$E_w = qa^2\sigma = (\sigma_0 qa^2/2)(\eta a/\delta_0 + \delta_0/\eta a) \quad (9)$$

Reduced wall energy $e_w = E_w/2a^3J_s^2$ will be

$$e_w = q[(\eta\sigma_0/4\delta_0 J_s^2) + (\sigma_0\delta_0/4\eta J_s^2 a^2)] \quad (10)$$

The total reduced energy of the two-domain configuration is $e = e_w + e_m$. Using (7) and (10), we can calculate e as a function of particle width a, domain wall width $y = \eta a$, and particle elongation q.

Rhodes and Rowlands [1954] have shown that the magnetostatic energy of a single-domain particle of width a and elongation q magnetized parallel to the elongation is

$$E_{SD} = 2J_s^2 vg(1, q) \quad (11)$$

where v is the particle volume. The reduced single-domain energy would be

$$e_{SD} = E_{SD}/2a^3J_s^2 = qg(1, q) \quad (12)$$

Following *Murthy et al.* [1971], the domain wall energy σ_0 of a 180° domain wall in magnetite can be estimated using the calculations of *Lilley* [1950]. For a domain wall parallel to (110),

$$\sigma_0 = 1.83(AK_1)^{1/2} \quad (13)$$

where A is the exchange constant. With $A = 1.5 \times 10^{-6}$ erg/cm [*Galt*, 1952] and $K_1 = 1.3 \times 10^5$ ergs/cm³ [*Fletcher and O'Reilly*, 1974], $\sigma_0 \simeq 0.8$ erg/cm². Domain wall width δ_0 can be estimated using *Lilley*'s [1950] results for Ni. *Lilley* [1950] found $\delta_0 = 2.06 \times 10^{-5}$ cm for a 180° wall parallel to (110) in Ni. Since $\delta_0 \propto (A/K_1)^{1/2}$, we can calculate δ_0 for magnetite by

$$\delta_0 = \delta_0'[(A/K_1)^{1/2}/(A'/K_1')^{1/2}] \quad (14)$$

where δ_0', A', and K_1' are the wall width, exchange constant, and anisotropy constant for Ni, and A and K_1 are the magnetite exchange and anisotropy constants. With $A' \simeq 10^{-6}$ erg/cm [*Martin*, 1967, p. 28], $K_1' = 4.5 \times 10^4$ ergs/cm³ [*Chikazumi*, 1964, p. 130], and $\delta_0' = 2.06 \times 10^{-5}$ cm, the domain wall width for magnetite is $\delta_0 = 1.5 \times 10^{-5}$ cm. This value is in good agreement with the estimate of 1.4×10^{-5} cm by *Morrish and Yu* [1955].

Using these input parameters along with $J_s = 480$ emu/cm³, we can calculate the threshold grain size d_0 for SD to two-domain transition by the following scheme:

1. Using (7) and (10), generate curves of total reduced energy e versus domain wall width $y = \eta a$ for various particle sizes a. Examples of these curves for a cubic magnetite particle at room temperature are shown in Figure 3. The point at which the e versus y curve is a minimum determines the preferred wall width for each particle size.

2. From the e versus y curves, determine the minimum reduced energy for each particle size and plot the minima versus particle size. This plot is shown in the inset of Figure 3.

3. Determine at which particle size the reduced energy minimum for the two-domain configuration falls below the SD reduced energy e_{SD}, which is determined from (12). Only for particle sizes where $e < e_{SD}$ will the two-domain configuration be energetically favorable. In the specific example shown in Figure 3, development of the two-domain configuration would be favored for particle sizes of >760 Å.

Thus the predicted d_0 is much less than the domain wall width in the extended medium δ_0. Although this 'squeezing' of the domain wall increases the wall energy, the large decrease in magnetostatic energy (compared to the SD configuration) makes the development of domain structure favorable in particle size $a < \delta_0$.

Superparamagnetic Threshold d_s

Transition to superparamagnetic behavior imposes a lower limit to the stable single-domain grain size range. This lower limit, d_s, can be calculated using *Néel*'s [1955] relaxation equation,

$$\tau = f_0^{-1} \exp(vh_cJ_s/2kT) \quad (15)$$

where τ is the relaxation time in seconds, f_0 is the frequency factor ($=10^9$ per second), v is the grain volume in cubic centimeters, h_c is the particle coercive force in oersteds, J_s is the saturation magnetization in electromagnetic units per

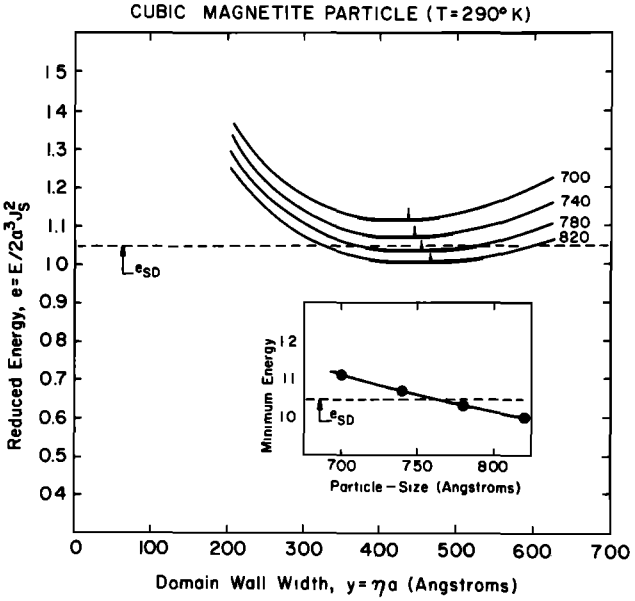

Fig. 3. Reduced energy e of two-domain configuration in cubic magnetite particles at 290°K as a function of domain wall width y ($=\eta a$) for several different particle sizes a. Each curve is labeled with its particle size at the right of the curve. Minimum energy for each particle size is indicated by the arrow. The single-domain reduced energy e_{SD} is indicated by the dashed line. The inset shows the minimum reduced energy versus particle size. The energy of the two-domain configuration falls below e_{SD} for particle sizes of >760 Å, indicating $d_0 \simeq$ 760 Å.

cubic centimeter, k is Boltzmann's constant, and T is the absolute temperature in degrees Kelvin. Néel's derivation of (13) was for the case of fine particles with uniaxial anisotropy. The factor ($vh_cJ_s/2kT$) is simply the energy barrier opposing spontaneous reversal of the magnetic moment. Simple substitution of h_c for particles with cubic anisotropy into (15) can lead to errors in relaxation time calculations. Thus *Bean and Livingston* [1959] suggest that (15) be rewritten to give

$$\tau = f_0^{-1} \exp (E_B/kT) \quad (16)$$

where E_B is the energy barrier opposing spontaneous reversal. Equation (16) is applicable to either cubic or uniaxial anisotropy.

For cubic magnetite particles (q = 1.0), magnetocrystalline anisotropy supplies the energy barrier opposing thermal activation of the magnetic moment. As the magnetic moment attempts to flip between adjacent [111] easy directions, it must surmount the energy barrier imposed by the intervening [110] direction. The resulting energy barrier in cubic magnetite particles will then be given by

$$E_B = E_K[110] - E_K[111] \quad (17)$$

where $E_K[110]$ and $E_K[111]$ are the magnetocrystalline anisotropy energies for the [110] and [111] directions of magnetization. $E_K[111] = -K_1v/3$, and $E_K[110] = -K_1v/4$, where K_1 is the first-order magnetocrystalline anisotropy constant. Thus $E_B = K_1v/12$, and (16) becomes

$$\tau = f_0^{-1} \exp (K_1v/12kT) \quad (18)$$

The threshold size for superparamagnetic behavior can be determined by substituting a critical relaxation time τ_s into (18) and solving for the critical cube edge d_s to obtain

$$d_s = [12kT \ln (f_0\tau_s)/K_1]^{1/3} \quad (19)$$

For elongated particles (q > 1.0), shape anisotropy will dominate the coercive force. The particle coercivity is given by

$$h_c = \Delta N J_s \quad (20)$$

where ΔN is the difference between the self-demagnetizing factors along the particle width and length. Shape anisotropy is uniaxial, and substitution of (20) into (15) yields

$$\tau = f_0^{-1} \exp (v\Delta N J_s^2/2kT) \quad (21)$$

For an elongated parallelepiped of square cross section the self-demagnetizing factor parallel to the elongation was determined by *Rhodes and Rowlands* [1954] as

$$N_q = 4g(1, q) \quad (22)$$

where $g(x, y)$ is again the Rhodes and Rowlands function given in (6). The self-demagnetizing factor perpendicular to the elongation is $N' = (4\pi - N_q)/2$, and the difference $\Delta N = N' - N_q$ will be

$$\Delta N = 2\pi - 6g(1, q) \quad (23)$$

Substituting (23) into (21) and solving for the critical length l_s yield

$$l_s = q(\{2kT \ln (\tau_s f_0)\}/\{qJ_s^2[2\pi - g(1, q)]\})^{1/3} \quad (24)$$

A rigorous derivation of the frequency factor f_0 for uniaxial anisotropy by *Brown* [1963*b*] has shown that f_0 is a function of v, h_c, J_s, and T. If the volume dependence of f_0 is included in (19) and (24), transcendental equations for d_s and l_s result. Fortunately, the superparamagnetic threshold sizes are insensitive to the exact value of f_0 [*Dunlop and West*, 1969]. Thus a constant frequency factor of 10^9/s has been used in the calculations to follow. The general problem of rigorous derivation of f_0 for cubic anisotropy has recently been discussed by *Aharoni* [1973].

Results and Discussion

Figure 4 illustrates the calculated SD grain size limits d_0 and d_s for cubic magnetite particles. The superparamagnetic threshold was calculated using (19) with τ_s = 100 s and 4 × 10^9 yr, while the SD to two-domain transition size was determined by the techniques described in the previous section. Temperature dependence was introduced by replacing the room temperature magnetic parameters with appropriate values at elevated temperature. The temperature dependence of J_s and K_1 was taken from *Pauthenet and Bochirol* [1951] and *Fletcher and O'Reilly* [1974], respectively. In order to determine the temperature dependence of domain wall energy and equilibrium thickness, σ_0 and δ_0, the temperature dependence of the exchange constant A is required. This temperature variation can be estimated by using the common approximation $A(T)/A(RT) = J_s(T)/J_s(RT)$, where $A(T)$ and $A(RT)$ are the exchange constants at temperature T and room temperature, while $J_s(T)$ and $J_s(RT)$ are the saturation magnetizations at T and at room temperature.

The calculated SD to two-domain threshold size d_0 in cubic magnetite particles at room temperature is 0.076 μm. Given the necessary approximations required in both the theoretical and experimental computations, this calculated upper limit to the single-domain grain size range in cubic magnetite is in good agreement with the experimental d_0 = 0.05 μm determined by *Dunlop* [1973*a*]. The results illustrated in Figure 4 indicate $d_s > d_0$ for T > 450°K. Thus no stable SD range exists for cubic magnetite particles at T > 450°K. Even at room temperature, d_s is only slightly below d_0, and only a very narrow SD range of $0.05 \le d \le 0.076$ μm is indicated. This very narrow SD range is also in good agreement with the experimental results of *Dunlop* [1973*a*]. In fact, *Dunlop* [1973*a*] pointed out that the proximity of the experimental d_0 and d_s sizes and the uncertainties involved allow for the possibility that no SD range exists for equant magnetite particles at room temperature.

Dunlop [1973*b*] observed that magnetite particles with average grain size less than 0.1 μm do not follow the TRM induction behavior predicted either by *Néel*'s [1955] two-domain

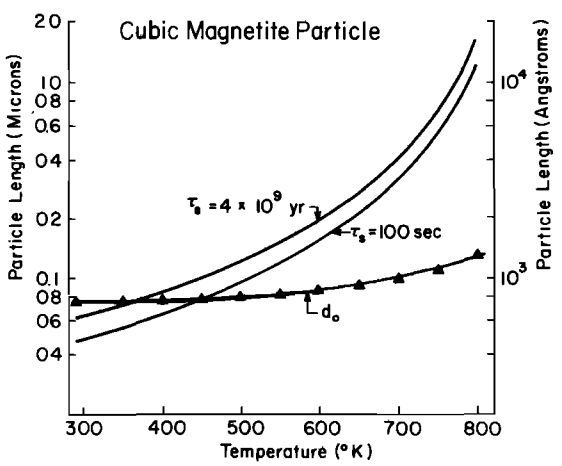

Fig. 4. Single-domain to two-domain transition size d_0 and superparamagnetic threshold d_s as a function of temperature for cubic magnetite particles. Here d_s is shown for critical relaxation times of 100 s and 4 × 10^9 yr. No stable SD range exists for T > 450°K.

model or by *Stacey*'s [1963] four-domain theory of pseudo-single-domain particles. *Dunlop* [1973*b*] attributed this disagreement to the development of a 'wavelike spin structure' in particles with $d < 0.1$ μm. Particles with grain size just above d_0 are thought to contain a domain wall which occupies a large proportion of the particle volume. Figure 3 shows that the preferred wall width increases with particle size, while the proportion of particle volume occupied by the domain wall decreases with increasing particle size. Thus the domain wall will occupy a large proportion of particle volume only for grains just above d_0. However, at d_0 (~760 Å) a wall width of ~450 Å is predicted for cubic particles. This wall would occupy ~60% of the particle volume. *Amar* [1958*b*] has shown that magnetic behavior of these two-domain particles is much different from that of larger multidomain grains. Thus it is not surprising that particles with $d < 0.1$ μm do not behave as predicted by the *Néel* [1955] or *Stacey* [1963] theories which treat the domain wall as a sharp plane which occupies an insignificant proportion of the particle volume. Therefore the two-domain theoretical treatment not only predicts SD limits in good agreement with experimental determinations but also predicts a spin configuration and wall width in small PSD particles which are consistent with experimental observations.

SD limits for square cross-section parallelepipeds with elongation q of 1.25 and 2.50 are shown in Figure 5. Superparamagnetic critical lengths l_s were calculated by using (24) with critical relaxation times τ_s of 100 s and 4×10^9 yr. Room temperature d_0 values of 0.11 and 0.42 μm are predicted for particles with q of 1.25 and 2.50, respectively. This increase in d_0 with elongation has been observed in previous theoretical

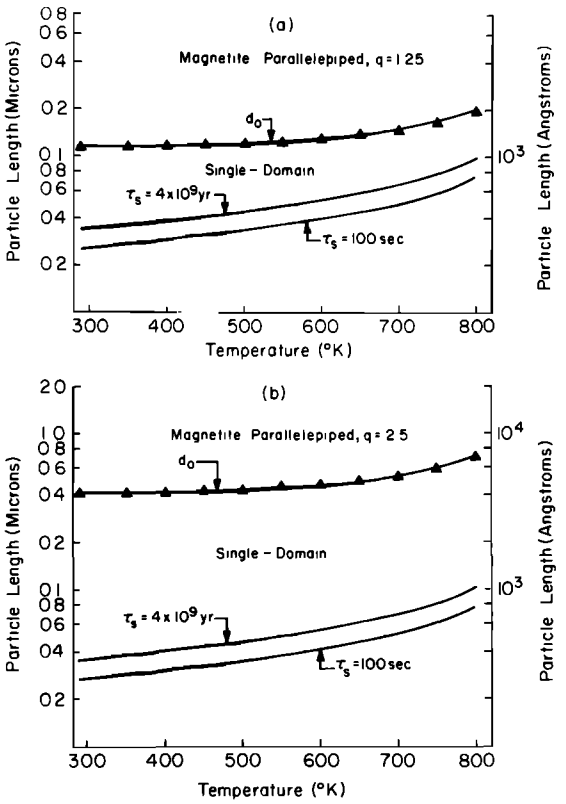

Fig. 5. Single-domain to two-domain transition length d_0 and superparamagnetic threshold l_s as a function of temperature for magnetite parallelepipeds with an elongation of (*a*) 1.25 and (*b*) 2.50. SP threshold lengths are calculated for critical relaxation times of 100 s and 4×10^9 yr. The stable SD range is between l_s and d_0.

SD calculations [*Strangway et al.*, 1968; *Evans and McElhinny*, 1969; *Murthy et al.*, 1971]. A lower demagnetizing factor parallel to the elongation produces lower magnetostatic energy in elongated SD grains than in cubic particles. Also the domain wall area in elongated particles is larger than that for cubic grains. Both of these factors lead to larger d_0 for elongated particles.

The most important result shown in Figure 5 is the development of a definite single-domain grain size range in the temperature range $290° \leq T \leq 800°$K. This SD range is in contrast to the results for cubic particles in which no single-domain range exists for $T > 450°$K. Grains with length l in the SD range $l_s < l < d_0$ will be very efficient and stable carriers of remanent magnetization.

In both Figures 4 and 5, d_0 increases with increasing temperature. This increase can be understood by considering the temperature dependence of the magnetic parameters required in the two-domain calculation. Both J_s and A (assumed proportional to J_s) decrease with increasing T while K_1 decreases as J_s^n with $n \simeq 8$ [*Fletcher and Banerjee*, 1969]. Domain wall energy, $\sigma_0 \propto (AK_1)^{1/2}$, will decrease as $J_s^{4.5}$ and wall width, $\delta_0 \propto (A/K_1)^{1/2}$, will increase as $J_s^{-3.5}$. Thus the increase in δ_0 and decrease in σ_0 nearly counterbalance, and the energy required to emplace a 180° domain wall decreases only slightly with increasing T. However, magnetostatic energy, which is the driving force favoring the two-domain configuration, decreases as J_s^2. Therefore a larger particle size is required before the magnetostatic energy of the single-domain configuration surpasses the total energy of the two-domain arrangement. Thus d_0 increases with increasing temperature.

The observed increase in d_0 with temperature implies quite different methods of TRM acquisition for particles on opposite sides of d_0 at room temperature. Single-domain grains with $l_s < l < d_0$ at 290°K will acquire TRM by the SD mechanism of passing through the SP to SD transition at their blocking temperature. However, the increase of d_0 with T indicates that some particles will be SD at elevated temperature but two-domain at room temperature. These particles would be in the pseudo-single-domain range. Although the TRM acquisition mechanism of PSD grains is not well understood, it is interesting to speculate that a transition to two-domain configuration from a single-domain state may be an important factor. Perhaps the statistical alignment of the SD state parallel to the ambient field is reflected by a preferential alignment of domain wall orientations or surface moments during the SD to two-domain transition. Any preferential alignment of the PSD moments during the transition would increase the TRM induction of these pseudo-single-domain particles.

The reduced energy e of two-domain magnetite particles with elongation $q = 2.5$ is shown as a function of wall width y in Figure 6. The critical length d_0 for SD to two-domain transition is ~4100 Å (~0.41 μm). At d_0 the wall width is ~400 Å, and the wall occupies ~25% of the 1600-Å particle width. The calculations indicate that domain walls in elongated two-domain particles occupy a smaller percentage of the particle width than walls in equant particles do. This observation is explained by the fact that the magnetization within the domain wall is forced to point perpendicular to the elongation. This direction will have a high demagnetizing factor, and thus the magnetostatic energy of the wall will be large. Therefore the wall is reduced in width in order to minimize the magnetostatic energy.

It is interesting to note that the domain wall width in two-domain particles at d_0 is nearly equal for cubic particles

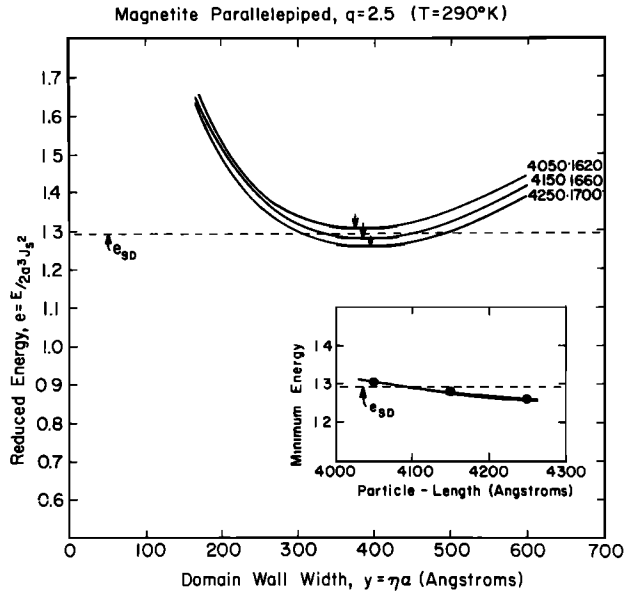

Fig. 6. Reduced energy e of the two-domain configuration at 290°K in magnetite parallelepipeds with an elongation of 2.5 as a function of domain wall width y ($=\eta a$). Length and width dimensions of the particle in angstroms are shown at the right of each curve, while the minimum energy of each particle size is indicated by the arrow. SD reduced energy e_{SD} is shown by the dashed line. Minimum reduced energy versus particle length is shown in the inset. Predicted d_0 for SD to two-domain transition occurs at a particle length of ~4100 Å.

(Figure 3) and parallelepipeds with elongation of 2.5 (Figure 6). In both cases the wall width is ~400 to 450 Å. This estimate of wall width is very helpful in evaluating the PSD theory recently proposed by *Stacey and Banerjee* [1974, p. 110]. This theory appeals to surface moments to explain the TRM induction of PSD grains. Since the surface:volume ratio of a particle with grain size d varies as d^{-1}, the d^{-1} dependence of TRM observed for PSD grains naturally follows from this surface moment theory. The surface moments range in magnitude from zero to an upper limit of μ_{max} given by

$$\mu_{max} = (2/\pi)d_0^2\delta J_s \qquad (25)$$

Physically, μ_{max} is the domain wall moment corresponding to a 180° wall which has thickness δ and area d_0^2. *Stacey and Banerjee* [1974, p. 110] used $\delta = 0.1$ μm and $d_0 = 0.5$ μm to derive $\mu_{max} = 7.6 \times 10^{-14}$ emu. However, if the d_0 and δ values of ~0.08 μm and ~0.05 μm determined above for cubic magnetites are used, (25) yields $\mu_{max} = 9.7 \times 10^{-14}$ emu. This value is in close agreement with the experimental value of 11.0×10^{-14} emu determined by *Dunlop et al.* [1974]. This close agreement may be simply fortuitous, but at least the present theoretical treatment is consistent with both the experimental data on TRM of pseudo-single-domain grains and the Stacey and Banerjee theory of PSD behavior.

The calculated single-domain grain size limits for magnetite at room temperature are summarized in Figure 7 as a function of axial ratio. In this figure, axial ratio is given as the inverse of elongation. Cubic particles are on the right side, while parallelepipeds of increasing elongation are toward the left. As mentioned previously, d_s and d_0 are in close proximity for cubic particles, and only a very narrow SD range exists. However, a substantial single-domain range exists for elongated particles. For a parallelepiped of elongation $q = 5.0$, $d_0 \simeq 1.4$ μm, while $l_s \simeq 0.05$ μm. It should be noted, however, that only the very elongated SD particles would be optically visible.

Single-domain limits for titanomagnetites can also be calculated by substituting the appropriate magnetic parameters needed in the d_0 and d_s calculations. The compositional dependence of J_s, A, and K_1 are required. Both Curie temperatures and K_1 have been determined for titanomagnetites $Fe_{3-x}Ti_xO_4$ of $x = 0.10, 0.18, 0.31, 0.56$, and 0.68 by *Syono* [1965]. The compositional variation at A can be estimated from the dependence of the Curie temperature on composition [*Chikazumi*, 1964, p. 186]. If A_0 is the exchange constant for magnetite (1.5×10^{-6} erg/cm), the exchange constant for a titanomagnetite of composition x is given by

$$A(x) = A_0 T_c(x)/T_{c0} \qquad (26)$$

where $T_c(x)$ is the Curie temperature of the titanomagnetite and T_{c0} is the Curie temperature of magnetite.

Results of the SD grain size calculations for titanomagnetites are shown in Figure 8 for cubic ($q = 1.0$) and elongated ($q = 2.5$) particles. The upper limit to SD behavior is seen to increase with increasing titanium content. This increase is primarily a reflection of the decreasing saturation magnetization J_s. For cubic particles the superparamagnetic threshold is dependent upon magnetocrystalline anisotropy. The initial increase of the absolute value of K_1 with Ti content is reflected by an initial decrease in d_s with increasing x. For $x > 0.1$ the magnitude of K_1 decreases with Ti content, and this decrease produces the observed increase in d_s for cubic particles. Since J_s decreases monotonically with x, the superparamagnetic threshold for elongated particles l_s increases steadily with increasing Ti content (Figure 8*b*). The most important observation in Figure 8 is that the SD range is wider and occurs at larger grain size as Ti content increases.

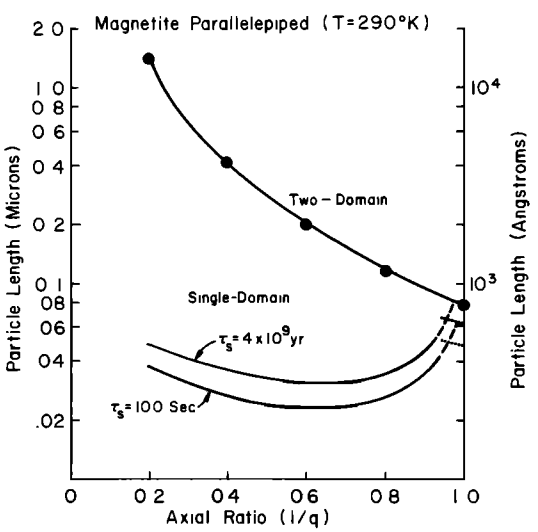

Fig. 7. Stable single-domain grain size range for magnetite parallelepipeds at 290°K as a function of axial ratio. The axial ratio is given as the inverse of elongation. Cubic particles appear at the right edge of the diagram and elongated particles are shown toward the left. The single-domain to two-domain transition length is shown by the line through the solid circles. Superparamagnetic threshold lengths l_s are shown for $\tau_s = 100$ s and 4×10^9 yr. The dashed portions of the l_s lines indicate the SP threshold length, assuming that shape anisotropy is the only source of coercivity. The dotted portions indicate the SP threshold if magnetocrystalline anisotropy is the only source of coercivity. The exact shape of l_s in this region will depend on the crystallographic direction of particle elongation. Stable SD behavior will be observed in the grain size region between l_s and d_0.

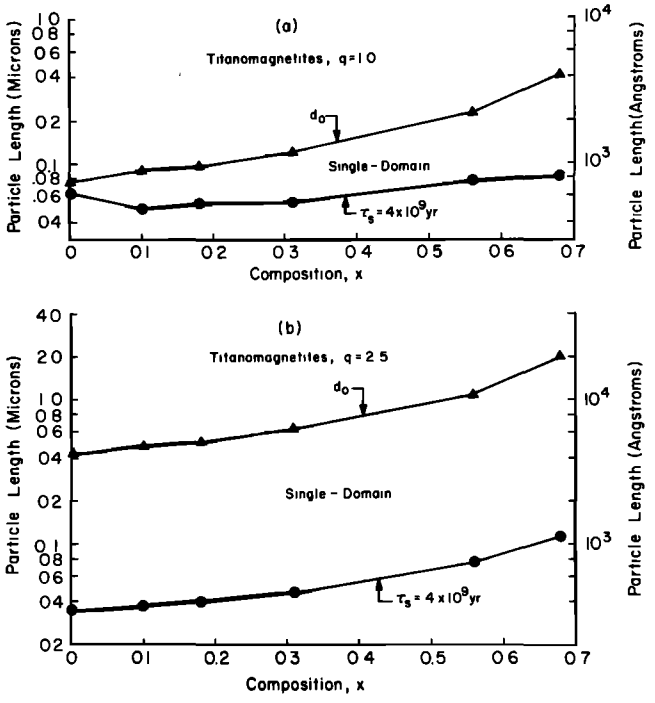

Fig. 8. Single-domain threshold sizes for titanomagnetites $Fe_{3-x}Ti_xO_4$ as a function of Ti content x for (*a*) cubic particles and (*b*) parallelepipeds of elongation 2.5. The SD to two-domain threshold d_0 is shown by the line through the solid triangles, while the SP threshold length l_s for critical relaxation time τ_s of 4×10^9 yr is indicated by the line through the solid circles.

Stacey [1963] predicted that d_0 would increase from magnetite toward ulvospinel (Fe_2TiO_4) as $J_s^{-1/2}$, while *Dunlop* [1973*a*] suggested $d_0 \propto J_s^{-3/2}$ for equant particles. A $J_s^{-1/2}$ dependence would predict $d_0 = 0.16$ μm for an $x = 0.55$ cubic titanomagnetite, while a $J_s^{-3/2}$ dependence predicts $d_0 = 0.8$ μm. The calculated d_0 shown in Figure 8*a* is 0.21 μm. The $J_s^{-1/2}$ dependence would also predict $d_0 = 0.8$ μm for $x = 0.55$ titanomagnetites with elongation $q = 2.5$, while the present calculations indicate $d_0 = 1.1$ μm. The discordance between the d_0 calculations of Figure 8 and those suggested by *Stacey* [1963] and *Dunlop* [1973*a*] simply indicate that d_0 for SD to two-domain transition is not a simple function of J_s. As with the temperature dependence of d_0 for pure magnetite, d_0 depends upon the domain wall width and energy δ_0 and σ_0 as well as the saturation magnetization J_s. Thus no simple dependence on J_s is expected.

It is also instructive to compare the theoretically derived d_0 values of Figure 8 with direct observations of domain structure. *Soffel* [1971] has used Bitter-pattern observations of $x = 0.55$ titanomagnetites in Tertiary basalts of Germany to estimate d_0. By extrapolating to submicroscopic sizes the observed trend of number of domains versus grain size, a d_0 value of ~0.7 μm was determined. It should be noted that this method does not consider the thinning of 180° domain walls in small two-domain particles. The present theoretical treatment indicates that two-domain structure will occur in grain sizes substantially smaller than the equilibrium wall width. Thus the extrapolation involved in *Soffel*'s [1971] method would overestimate d_0. Direct comparison of theory and observation is further complicated by the fact that the degree of elongation of the observed particles is difficult to determine. Nevertheless, the calculated d_0 values for $x = 0.55$ of ~0.2 μm for cubic particles and ~1.0 μm for $q = 2.5$ particles bracket the $d_0 \simeq 0.7$ μm extrapolation by *Soffel* [1971]. Thus the theoretical results shown in Figure 8 are consistent with the available observations.

Direct evaluation of the importance of SD magnetite and titanomagnetite in carrying stable NRM could be accomplished by comparing the grain size distributions of igneous rocks with the theoretical single-domain grain size limits derived above. Such a comparison is made difficult by the paucity of grain size observations extending into the submicron range. However, several lines of evidence suggest that the percentage of magnetites in the SD range is significant. *Larson et al.* [1969] found several grain size distributions for opaques in igneous rocks which appeared to peak in the submicron range. Also exsolution patterns produced by deuteric oxidation or simple unmixing can yield effective grain sizes much less than the optically observed grain size [*Evans and Wayman*, 1974]. Electron microscope observations of opaque grains in igneous rocks have helped to extend observations into the submicron range. *Evans and Wayman* [1970] found a grain size distribution in a magnetically stable intrusive rock which peaked at ~¼ μm. If these grains exhibit any elongation, a large percentage of the magnetites would fall within the SD limits of Figure 7. The larger grain size range and larger size at which single-domain behavior is expected for titanomagnetites greatly increase the probability that SD particles dominate the NRM of titanomagnetite-bearing rocks. Electron microscope observations of titanomagnetites in pillow basalts dredged from the mid-Atlantic Ridge have revealed the presence of opaque grains which would easily fall within the single-domain limits of Figure 8 [*Evans and Wayman*, 1972]. Additional high-resolution observations of opaque grains are badly needed in order to evaluate further the importance of SD magnetites and titanomagnetites in carrying stable NRM of igneous rocks. However, the limited available observations do indicate the presence of single-domain magnetite in the magnetically stable rocks which have been investigated.

Conclusion

The two-domain configuration of *Amar* [1958*a*] is designed for parallelepiped-shaped particles and is thus more applicable to fine-grained magnetites in igneous rocks than the *Morrish and Yu* [1955] circular spin configuration which considers only ellipsoidal particles. Neglected magnetocrystalline anisotropy energy and magnetostatic energy arising from confining the circular spin configuration to fine particles bounded by crystal faces are significant contributors to the energy of the circular spin arrangement. Application of the *Morrish and Yu* [1955] calculations to magnetite particles in igneous rocks amounts to neglecting these important energy contributions. A transition from single-domain to circular spin configuration at the SD threshold size d_0 is also in conflict with experimental observations of TRM induction in submicron PSD magnetites.

Application of the *Amar* [1958*a*] two-domain theory to cubic magnetite particles indicates that a SD to two-domain transition at d_0 is consistent with experimental observations. Given the necessary approximations in both theory and experiment, the calculated d_0 of 0.076 μm is in good agreement with the experimental value of 0.05 μm [*Dunlop*, 1973*a*]. For cubic particles just above d_0 a two-domain configuration is predicted in which a 180° domain wall occupies ~60% of the particle volume. This result is also in agreement with the experimental observations of TRM in submicron PSD grains [*Dunlop*, 1973*b*]. The success of the two-domain configuration in predicting both d_0 for cubic particles and a domain structure

for submicron PSD particles which are in agreement with experiment argues strongly for the physical reality of a SD to two-domain transition at d_0. Thus the upper limit to SD behavior in magnetite particles of igneous rocks is imposed by transition to a two-domain configuration in which a 180° domain wall occupies a significant proportion of the particle volume. This result is an important reconciliation between theory and experiment.

Calculations of the stable SD grain size range were accomplished by determining the superparamagnetic threshold d_s by *Néel*'s [1955] relaxation equation and by determining the single-domain threshold d_0 by the technique of *Amar* [1958*a*]. Major results of the stable SD grain size calculations for magnetite and titanomagnetite are as follows:

1. For cubic magnetite particles the SD range is very narrow and occurs at very small grain size. At room temperature, $d_s \simeq 0.05$ μm, and $d_0 \simeq 0.076$ μm; d_s increases rapidly with increasing temperature and no stable SD range exists for $T >$ 450°K.

2. The stable SD range for magnetite increases with increasing particle elongation. For a parallelepiped with length:width ratio of 5:1, stable SD behavior is expected for lengths between ~0.05 and ~1.4 μm. Only very elongated SD magnetites will be optically visible.

3. Both single-domain threshold size d_0 and the stable SD range for titanomagnetites increase with Ti content. For cubic particles of $x = 0.6$ composition, $d_0 \simeq 0.3$ μm, while $d_s \simeq 0.08$ μm. The calculated d_0 values for $x = 0.55$ titanomagnetites are consistent with the observations of *Soffel* [1971].

Direct evaluation of the importance of SD magnetites and titanomagnetites in carrying stable NRM of igneous rocks is made difficult by the limited availability of high-resolution observations of opaque grain size distributions. However, electron microscope investigations have revealed the presence of magnetites in magnetically stable intrusive rocks which would fall within the calculated SD limits. The calculations of this paper along with experimental investigations of the magnetic behavior of NRM in igneous rocks comprise a growing body of data which suggests that stable NRM in igneous rocks is dominated by single-domain and/or submicron pseudo-single-domain grains.

APPENDIX 1

Consider the circular spin configuration in a prolate ellipsoid elongated parallel to [001]. The spins lie in the (100) plane and describe circles about the [001] direction. This particular example is chosen because the calculation is much simpler than for other orientations. As the magnetization rotates in the (100) plane, it passes through four [100] directions and four [110] directions in 360°. The easy directions of magnetization in magnetite are the [111] directions for which the anisotropy energy per unit volume is $e_K[111] = -K_1/3$, where K_1 is the absolute value of the first-order magnetocrystalline anisotropy constant. The neglected anisotropy energy of the circular spin configuration will be $e_K - e_K[111]$, where e_K is the calculated anisotropy energy of the configuration.

The anisotropy energies of the [100] and [110] directions are 0 and $-K_1/4$, respectively. Thus $e_K[100] - e_K[111] = K_1/3$, and $e_K[110] - e_K[111] = K_1/12$. If we use standard spherical coordinates with $\theta = 0°$ along [001] and ϕ in the (100) plane with $\phi = 0$ at the point where the magnetization is parallel to [110], the ϕ dependence of the anisotropy energy $e_K(\phi)$ is given by

$$e_K(\phi) = K_1/12 + (K_1/4)\sin^2(2\phi) \tag{27}$$

The total magnetocrystalline energy of the configuration is simply the volume integral of $e_K(\phi)$. This integral is

$$E_K = \int_0^{\pi} \int_0^{g(\theta)} \int_0^{2\pi} e_K(\phi) r^2 \sin\theta \, d\phi \, dr \, d\theta \tag{28}$$

where

$$g(\theta) = ab/(b^2 \sin^2\theta + a^2 \cos^2\theta)^{1/2} \tag{29}$$

Here $g(\theta)$ is the equation of the prolate ellipsoidal surface, a is the semiminor axis, and b is the semimajor axis. The integration yields

$$E_K = 10\pi K_1 a^2 b/36 \tag{30}$$

The magnetocrystalline energy per unit volume is

$$e_K = E_K/(4\pi a^2 b/3) = 5K_1/24 \tag{31}$$

APPENDIX 2

The complete expression of the *Rhodes and Rowlands* [1954] function is

$$\begin{aligned} F(p, q) = {} & (p^2 - q^2)\sinh^{-1}[1/(p^2 + q^2)^{1/2}] \\ & + p(1 - q^2)\sinh^{-1}[p/(1 + q^2)^{1/2}] \\ & + pq^2 \sinh^{-1}(p/q) + q^2 \sinh^{-1}(1/q) \\ & + 2pq \tan^{-1}[(q/p)(1 + p^2 + q^2)^{1/2}] \\ & - \pi pq - (\tfrac{1}{3})(1 + p^2 - 2q^2)(1 + p^2 + q^2)^{1/2} \\ & + (\tfrac{1}{3})(1 - 2q^2)(1 + q^2)^{1/2} \\ & + (\tfrac{1}{3})(p^2 - 2q^2)(p^2 + q^2)^{1/2} + (\tfrac{2}{3})q^3 \end{aligned} \tag{32}$$

Acknowledgments. We thank D. J. Dunlop for suggesting an analysis of single-domain limits based on the two-domain configuration developed by H. Amar. We also thank William Fuller Brown for helpful discussions of magnetostatic principles and calculations. This research was funded by NSF grant GA-35249. Contribution 605 of the Department of Geosciences, University of Arizona.

REFERENCES

Aharoni, A., Relaxation time of superparamagnetic particles with cubic anisotropy, *Phys. Rev. B., 7,* 1103–1107, 1973.

Amar, H., On the width and energy of domain walls in small multidomain particles, *J. Appl. Phys., 28,* 732–733, 1957.

Amar, H., Size dependence of the wall characteristics in a two-domain iron particle, *J. Appl. Phys., 29,* 542–543, 1958*a*.

Amar, H., Magnetization mechanism and domain structure of multidomain particles, *Phys. Rev., 111,* 149–153, 1958*b*.

Bean, C. P., and J. D. Livingston, Superparamagnetism, *J. Appl. Phys., 30,* 120S–129S, 1959.

Brown, W. F., Jr., *Micromagnetics,* 143 pp., John Wiley, New York, 1963*a*.

Brown, W. F., Jr., Thermal fluctuations of a single-domain particle, *Phys. Rev., 130,* 1677–1686, 1963*b*.

Chikazumi, S., *Physics of Magnetism,* 554 pp., John Wiley, New York, 1964.

Dickson, G. O., C. W. F. Everitt, L. G. Parry, and F. D. Stacey, Origin of thermoremanent magnetization, *Earth Planet. Sci. Lett., 1,* 222–224, 1966.

Dunlop, D. J., Magnetite: Behavior near the single-domain threshold, *Science, 176,* 41–43, 1972.

Dunlop, D. J., Superparamagnetic and single-domain threshold sizes in magnetite, *J. Geophys. Res., 78,* 1780–1793, 1973*a*.

Dunlop, D. J., Thermoremanent magnetization in submicroscopic magnetite, *J. Geophys. Res., 78,* 7602–7613, 1973*b*.

Dunlop, D. J., and G. F. West, An experimental evaluation of single-domain theories, *Rev. Geophys. Space Phys., 7,* 709–757, 1969.

Dunlop, D. J., F. D. Stacey, and D. E. W. Gillingham, The origin of thermoremanent magnetization: Contributions of pseudo-single-domain magnetic moments, *Earth Planet. Sci. Lett., 21,* 288–294, 1974.

Evans, M. E., Single-domain particles and TRM in rocks, *Commun. Earth Sci. Geophys., 2,* 139–148, 1972.

Evans, M. E., and M. W. McElhinny, An investigation of the origin of stable remanence in magnetite-bearing igneous rocks, *J. Geomagn Geoelec., 21,* 757–773, 1969.

Evans, M. E., and M. L. Wayman, An investigation of small magnetic particles by means of electron microscopy, *Earth. Planet. Sci Lett., 9,* 365–370, 1970.

Evans, M. E., and M. L. Wayman, The mid-Atlantic Ridge near 45° N, 9, An electron microscope investigation of the magnetic minerals in basalt samples, *Can. J. Earth Sci., 9,* 671–678, 1972.

Evans, M. E., and M. L. Wayman, An investigation of the role of ultra-fine titanomagnetite intergrowths in palaeomagnetism, *Geophys. J. Roy. Astron. Soc., 36,* 1–10, 1974.

Evans, M. E., M. W. McElhinny, and A. C. Gifford, Single domain magnetite and high coercivities in a gabbroic intrusion, *Earth Planet. Sci. Lett., 4,* 142–146, 1968.

Fletcher, E. J., and S. K. Banerjee, High temperature dependence of single crystal anisotropy constants of titanomagnetites (abstract), *Eos Trans. AGU, 50,* 132, 1969.

Fletcher, E. J., and W. O'Reilly, Contribution of Fe^{2+} ions to the magnetocrystalline anisotropy constant K_1 of $Fe_{3-x}Ti_xO_4$ ($0 < x < 0.1$), *Proc. Phys. Soc. London Solid State Phys., 7,* 171–178, 1974.

Galt, J. K., Motion of a ferromagnetic domain wall in Fe_3O_4, *Phys. Rev., 85,* 664–669, 1952.

Hargraves, R. B., and W. M. Young, Source of stable remanent magnetism in Lambertville diabase, *Amer. J. Sci., 267,* 1161–1177, 1969.

Kittel, C., Physical theory of ferromagnetic domains, *Rev. Mod. Phys., 21,* 541–583, 1949.

Larson, E., M. Ozima, M. Ozima, T. Nagata, and D. Strangway, Stability of remanent magnetization of igneous rocks, *Geophys. J. Roy. Astron. Soc., 17,* 263–292, 1969.

Lilley, B. A., Energies and widths of domain boundaries in ferromagnetics, *Phil. Mag., 41,* 792–813, 1950.

Martin, D. H., *Magnetism in Solids,* 452 pp., Iliffe, London, 1967.

Morrish, A. H., *The Physical Principles of Magnetism,* 680 pp., John Wiley, New York, 1965.

Morrish, A. H., and S. P. Yu, Dependence of the coercive force on the density of some iron oxide powders, *J. Appl. Phys., 26,* 1049–1055, 1955.

Moskowitz, R., and E. Della Torre, Theoretical aspects of demagnetization tensors, *IEEE Trans. Magn., 2,* 739–744, 1966.

Murthy, G. S., M. E. Evans, and D. I. Gough, Evidence for single-domain magnetite in the Michikamau anorthosite, *Can. J. Earth Sci., 8,* 361–370, 1971.

Néel, L., Théorie du trainage magnétique des ferromagnétiques au grains fin avec applications aux terres cuites, *Ann. Geophys., 5,* 99–136, 1949.

Néel, L., Some theoretical aspects of rock-magnetism, *Advan. Phys., 4,* 191–243, 1955.

Parry, L. G., Magnetic properties of dispersed magnetite powders, *Phil. Mag., 11,* 303–312, 1965.

Pauthenet, R., and L. Bochirol, Aimantation spontaneé des ferrites, *J. Phys. Radium, 12,* 249–251, 1951.

Rhodes, P., and G. Rowlands, Demagnetizing energies of uniformly magnetized rectangular blocks, *Proc. Leeds Phil Lit. Soc., Sci. Sect., 6,* 191–210, 1954.

Soffel, H., The single domain-multidomain transition in natural intermediate titanomagnetites, *Z. Geophys., 37,* 451–470, 1971.

Stacey, F. D., The physical theory of rock magnetism, *Advan. Phys., 12,* 45–133, 1963.

Stacey, F. D., and S. K. Banerjee, *The Physical Principles of Rock Magnetism,* 195 pp., Elsevier, New York, 1974.

Strangway, D. W., E. E. Larson, and M. Goldstein, A possible cause of high magnetic stability in volcanic rocks, *J. Geophys. Res., 73,* 3887–3895, 1968.

Syono, Y., Magnetocrystalline anisotropy and magnetostriction of Fe_3O_4-Fe_2TiO_4 series—With special application to rock magnetism, *Jap. J. Geophys., 4,* 71-143, 1965.

(Received September 30, 1974;
revised February 10, 1975;
accepted February 27, 1975.)